

Using Machine Learning for the Performance-Based Seismic Assessment of Slope Systems

Chenyang Liu¹; Jorge Macedo, Ph.D.²; and Farahnaz Soleimani, Ph.D.³

¹Graduate Student Researcher, Dept. of Civil and Environmental Engineering, Georgia Institute of Technology, Atlanta. Email: cliu662@gatech.edu

²Assistant Professor, Dept. of Civil and Environmental Engineering, Georgia Institute of Technology, Atlanta. Email: jorge.macedo@ce.gatech.edu

³Dept. of Civil and Environmental Engineering, Georgia Institute of Technology, Atlanta. Email: farahnazsoleimani@gmail.com

ABSTRACT

Engineers often use analytical procedures, which estimate the amount of seismically induced slope displacements (D), to evaluate the seismic performance of earth structures and natural slopes. These procedures often use as inputs slope properties, earthquake parameters, and ground motion intensity measures (IM_s). In this study, we propose a new set of machine learning (ML) based models to estimate D using the NGA-West2 shallow crustal ground motion database. Our findings suggest that the most efficient features to evaluate the seismic performance of slope systems are the slope's yield coefficient (k_y), its fundamental period (T_s), the earthquake magnitude (M_w), the peak ground velocity (PGV), and the degraded spectral acceleration at 1.3 T_s . We assess the performance of the proposed models by evaluating cross-validation errors, their predictive performance in case histories, and comparisons against existing models. Based on the assessments, we recommend 6 ML-based models to estimate D in engineering practice.

INTRODUCTION

The seismic performance assessment of slope systems is typically performed by: (a) Newmark-based slope displacement analyses, (b) pseudo-static slope stability analyses, and (c) advanced numerical procedures, such as finite elements or finite differences (Macedo et al. 2020). Even though advanced numerical analyses are increasingly used in practice, method (a) is preferred in engineering practice for its simplicity, particularly in the preliminary design stages. Method (b) is also still used in practice mainly because some regulators explicitly request its application as part of the evaluation of the seismic stability of slope systems, at least in projects with a low associated risk (e.g., MEM, 1997; Ministerio de Minería, 2007; APEGBC, 2010; FHWA, 2011; Moreno and Kendall, 2019; Macedo and Candia, 2020). Newmark-based slope displacement analyses are typically based on seismic sliding block displacement analysis, which estimates the amount of seismically-induced slope displacements (D). When a D model is developed, Newmark-based approaches are typically used with a ground motion database to generate D realizations, which are subsequently used to develop semiempirical D models. A fundamental input for developing a D model is the selection of efficient parameters that can explain the trends in D . These parameters are often selected among candidates such as the earthquake magnitude (M_w), rupture distance ($ClstD$), and ground motion intensity measure parameters (IM_s). Previous efforts have typically used fixed functional forms consisting of polynomials of $\ln(IM)$ (often first or second-degree polynomials) to select efficient IM_s by calculating the standard deviation of linear regressions where the IM is changed iteratively,

typically considering only one IM at the time (e.g., Bray and Travararou, 2007). As opposed to traditional approaches, several well-established machine-learning (ML)-based procedures have been developed to guide the selection of efficient features to estimate D in a more holistic manner. In addition, ML-based models have the potential to better capture the complex relationships between the input and response variables without restriction to relatively simple functional forms as in traditional models. Thus, their use in performance-based earthquake engineering is appealing (Xie et al., 2020). There have been relatively few previous studies in the context of the estimation of seismically-induced displacements in slope systems. For example, Wang et al. (2020) built a predictive model based on the extreme gradient boosting (XGboost) algorithm using a dataset containing 43,832 seismic slope displacements. They used three different sets of input features: peak ground acceleration (PGA), peak ground velocity (PGV); PGA and arias intensity (I_a); and PGA , PGV and I_a , and found that their XGBoost-based models were superior to the traditional semiempirical counterparts. More recently, Cho (2020) developed a multi-layer perceptron network based on a database with 42,040 D realizations. In terms of the input features, they considered the slope's yield coefficient (k_y), initial fundamental period (T_s), and PGV . Compared to the traditional models developed by Cho and Rathjé (2020) with a similar database, the proposed multi-layer perceptron model improved the prediction of median displacements. Thus, these previous studies highlight the potential benefits of ML-based procedures against their traditional counterparts to estimate D . Although these models are a step forward in performance-based earthquake engineering, they also have some limitations. For example, the model in Wang et al. (2020) is nonparametric, which may introduce challenges in terms of interpretability (Hastie et al., 2009). Moreover, the previous referred models have not been evaluated against case histories, they did not use an extensive ground motion database (e.g., the NGA-West2 database Bozorgnia et al., 2014 used in this study), and they used IM_s inherited from traditional semiempirical models without a systematic feature selection. In this study, ML-based procedures are used for selecting efficient parameters used to develop new ML-based models to estimate D for regions affected by shallow crustal earthquakes. The considered machine-learning techniques include multiple feature selection techniques and regression models. The ML-based procedures developed in this study consider a large ground motion database (i.e., the NGA-West2 database), both parametric and nonparametric models to balance the tradeoff between model interpretability and prediction performance (Hastie et al., 2009), and case histories as an additional metric to evaluate the performance of the formulated models.

DATABASE

We use the NGA-West2 database for shallow crustal earthquakes, which contains 21,332 three-component ground motion recordings (Bozorgnia et al., 2014). For the estimation of D , ground motion records are chosen from earthquakes with M_w from 5 to 7.9 at ClstD less than 200 km and site classes A, B, C, and D (ICC, 2015). A total of 6,711 ground motion records (with each record having two horizontal components) are employed to generate the D data. Figure 1 shows the distribution of M_w and ClstD for the ground motions used in this study. We employ the fully coupled, nonlinear, deformable stick-slip sliding model proposed by Rathjé and Bray (1999), with the modifications in Macedo (2017) and Macedo et al. (2017) to estimate seismically-induced displacements. In this model, the dynamic response of the deformable sliding mass is captured by an equivalent-linear viscoelastic modal analysis that uses strain-dependent material properties. We used the ground motions in the database as inputs to the fully

coupled stick-slip model. The fully coupled stick-slip sliding model is characterized by its k_y , ranging from 0.01 to 0.8, and its T_s , ranging from 0 to 2. The properties assigned to the model (k_y and T_s) represent a wide range of natural earth slopes, earth dams, and solid-waste landfills. Then each ground motion recording in the database is applied to the base of the fully coupled stick-slip model to calculate D values. The D values calculated from the two horizontal components are averaged. More details on the slope properties and calculation of D values can be found in Macedo et al. (2021).

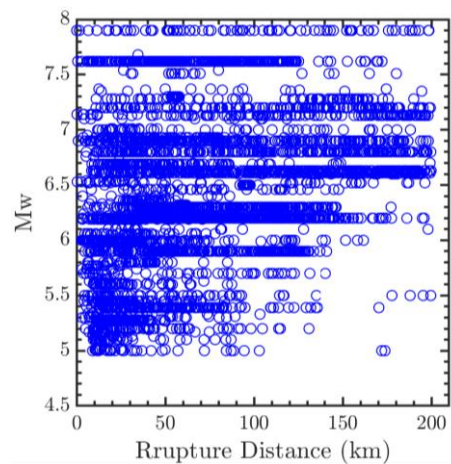


Figure 1. Magnitude and distance distribution for the ground motions recordings used in this study.

The list of the collected features that are considered as candidates to estimate D include slope properties, earthquake parameters, and IM_s (calculated as the geometric mean of the two horizontal recorded components). Specifically, we considered 21 features: k_y , T_s , significant duration (d_{5-95}), M_w , $ClstD$, V_{s30} (time-averaged shear wave velocity in the top 30m), I_a , PGA , PGV , and $Sa(nT_s)$ (spectral acceleration at a degraded period equal to nT_s , with $n = 1.0, 1.1, 1.2, 1.3, 1.4, 1.5, 1.6, 1.7, 1.8, 2.0, 2.5, 3.0$). Following common ML practices (e.g., Hastie et al., 2009), we divide the database into a training-validation set and a test set. The training-validation set (contains 90% of the entire data) is used to train the model parameters, and if necessary (i.e., for ML models with hyperparameters), is further split into 10 cross-validation folds for the optimization of hyperparameters. The remaining 10% data are used as the test set to compare the predictive performance of the models. Additional details on the cross-validations can be found in Macedo et al. (2021).

FEATURE SELECTION

The 21 parameters described previously are used as feature candidates to develop D predictive models. Sparse regression algorithms (Forward Stepwise Regression (FSS), LASSO (Least Absolute Shrinkage and Selection Operator), and Random Forest), are implemented to determine an appropriate combination of features to explain D . Detailed explanation of the feature selection algorithms can be found in Krishnapuram et al. (2013), Cawley et al. (2007), Hastie et al. (2009), and Macedo et al. (2021). The feature selection results are assessed using the training-validation set with 10-fold cross-validation. Figure 2, obtained from FSS, displays the

prediction accuracy averaged across 10 validation folds for each number of features. Figure 2 shows that as the number of features increases, the prediction accuracy increases rapidly, but soon bounded by a threshold of around 75%. The gap between 100% and 75% corresponds to the inherent noises and existing nonlinearity in the dataset. According to this graph, five features (k_y , T_s , M_w , PGV , and $Sa(1.3 T_s)$) can be selected by FSS as the optimum number since the improvement of prediction power is insignificant after that. The LASSO approach tends to select as many features as possible to achieve the minimum mean squared error (MSE), hence, all features excepted d_{5-95} , $Sa(1.7 T_s)$, and I_a (i.e., totally 18 features) are selected. LASSO results are used as corroboration for feature selection of the other techniques and provide a benchmark for the performance evaluation of other approaches. For random forest, six features (k_y , PGV , T_s , $Sa(1 T_s)$, $Sa(1.1 T_s)$, and M_w) with highest importance are selected. The features selected by Random Forest and Forward Stepwise Selection are both subsets of the 18 features selected by LASSO. The performance of the three feature selection techniques is compared with a full linear model (including all features) in terms of the prediction accuracy and MSE on the test set. Both the full linear and the LASSO model which has a large number of features, show no significant improvement in performance compared to other cases. Random Forest performed best among the applied techniques, showing the highest prediction accuracy and lowest MSE. The Forward Stepwise Selection technique with five features performed close to Random Forest. Besides, Forward Selection exhibits a comparable prediction accuracy and MSE to those of the full linear model. In summary, both Random Forest and Forward Stepwise Selection registered that optimal efficiency (i.e., high prediction accuracy and low MSE) can be achieved considering a reduced number of features. Although Random Forest identified six features as the most influential predictors in estimating D , the Forward Stepwise technique revealed no notable improvement in the prediction power beyond five features, as demonstrated in Figure 2. In addition, in terms of the features selected by Random Forest, two of them are highly correlated (i.e., $Sa(1.0 T_s)$, and $Sa(1.1 T_s)$). Thus, the selected influential features are k_y , T_s , M_w , PGV , and $Sa(1.3 T_s)$, which will be used in the subsequent sections to propose D predictive models.

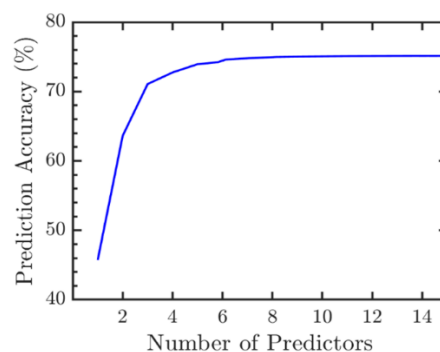


Figure 2. Forward Selection: averaged prediction accuracy vs. the number of features.

PREDICTIVE MODELS

Based on the features selected using the feature selection algorithms, we implement 19 machine-learning-based models (M1 to M19) with different degrees of flexibility to estimate D , which are summarized in Table 1 (Check Macedo et al., 2021 for detailed model definitions). The hyperparameters of the ML models are optimized through a grid-search method based on

their performance in the training-validation set (more details on hyperparameter optimization can be found in Macedo et al., 2021). Finally, the performance of different ML models with optimized parameters is evaluated based on their prediction accuracy and MSE on the test set, as summarized in Table 1. The main outcomes include: (a) nonlinear models and second-order polynomials (i.e., M4 to M19) show the highest accuracy and the lowest MSE, models that used the full set of features ranked first; however, models that used five features ranked close. (b) Principal component regression (PCR) uses more principal components than partial least square regression (PLSR); however, it does not exhibit better performance. The variation in the response variable, which is not captured by PCR, causes the lower efficiency of this approach. Overall, PLSR and PCR do not provide models with good performance for the database considered in this study. (c) Polynomial models with lower orders have better performance than polynomials with higher orders since the higher-order polynomials are more likely to overfit the data in the training process. (d) The tree-based methods (M4 to M7) perform similarly in terms of prediction accuracy and MSE.

In summary, the top-ranked candidate predictive models (models with five features, which are preferred due to their simplicity) based on the MSE and prediction accuracy are M18 (Gaussian Kernel), M4 (Bagging and Boosting), M6 (Random Forest), M16 (2nd order fully polynomial regression model), M17 (Multi-order polynomial regression model), M15 (2nd order polynomial regression model with linear and interactive terms), and M1 (Generalized Linear regression model). All these models (except M1) have an MSE lower than 0.3. To compare these models with an existing model that is commonly used in practice, we have also calculated the MSE for the Bray and Macedo (2019) model (BM2019) (this model is an update of the Bray and Travararou (2007) model that has been widely used in engineering practice), which is 0.51 and larger than most of the MSE in the models listed above. Figures 3 and 4 show illustrative trends for selected models (models M16 and M17); the trends are presented in terms of variations of k_y , T_s , $S_a(1.3 T_s)$, and M_w (calculation of $S_a(1.3 T_s)$) and more plots for other models are detailed in Macedo et al., 2021). In general, we observed that most of the models with low MSE show consistent qualitative trend patterns as those in the BM2019 model. D increases initially with the increase of T_s and then decreases as T_s keeps increasing; D decreases with the increase of k_y , and finally, D increases with the increase of M_w and $S_a(1.3 T_s)$.

PERFORMANCE OF THE PROPOSED MODELS IN CASE HISTORIES

This section evaluates the performance of the models proposed in the previous sections considering the case histories compiled by Bray and Travararou (2007). Table 2 presents the details of the case histories, which are associated with the observed seismic performance of different slope systems (e.g., earth dams and waste landfills) that were affected by shallow crustal earthquakes. We have used the mean squared prediction error (MSPE, see Macedo et al., 2021) to indicate the predictive performance on case histories. Figure 5 present the MSPEs for the different models considered in this study when they are evaluated against case histories. Figure 6 shows the comparison of predicted D values from the selected models with observed D values in the case histories (See a full list of plots for all models in Macedo et al., 2021). In addition, the bars in Figure 6 correspond to 95% confidence intervals. Models M1, M17, M8, M16, M15, and M12, have MSPE values that vary between 37 to 47, featuring a good performance against case histories. These models predict a good seismic performance (small D) when the observed performance was good, and they also predict potential damage (large D)

when the observed D values were large. Models M6 and M18 have MSPE values of 128 and 183, respectively. These models are also capable of distinguishing between different levels of seismic performance, but their MSPE values are inflated by their conservative predictions on case histories 5 and 6. The other models, M13 and M14, which are polynomials of 3rd and 4th order, have quite large MSPEs, and they present a poor performance. These models are very sensitive to changes in the input variables due to their high-order polynomials.

Table 1. Performance comparison of the developed predictive models

| Models | Algorithms | Features used | Prediction Accuracy | MSE |
|--------|---|---|---------------------|-------|
| M1 | Generalized Linear Model | 5 features chosen previously | 0.730 | 0.384 |
| M2 | Partial Least Square Regression | 3 principal components | 0.723 | 0.403 |
| M3 | Principal Component Regression | 5 principal components | 0.691 | 0.498 |
| M4 | Bagging and Boosting | 5 features chosen previously | 0.866 | 0.227 |
| M5 | Bagging and Boosting | All 21 features | 0.904 | 0.161 |
| M6 | Random Forest | 5 features chosen previously | 0.847 | 0.244 |
| M7 | Random Forest | All 21 features | 0.887 | 0.197 |
| M8 | Polynomial 2 nd order (w/o interactive variables) | Repeated feature selection for this model format | 0.697 | 0.486 |
| M9 | Polynomial 3 rd order (w/o interactive variables) | Repeated feature selection for this model format | 0.651 | 0.635 |
| M10 | Polynomial 2 nd order (combination of linear and interactive variables) | Repeated feature selection for this model format | 0.824 | 0.170 |
| M11 | Polynomial 2 nd order (combination of linear, squared and interactive variables) | Repeated feature selection for this model format | 0.847 | 0.126 |
| M12 | Polynomial 2 nd order (w/o interactive variables) | 5 features chosen previously | 0.687 | 0.517 |
| M13 | Polynomial 3 rd order (w/o interactive variables) | 5 features chosen previously | 0.630 | 0.715 |
| M14 | Polynomial 4 th order (w/o interactive variables) | 5 features chosen previously | 0.570 | 0.949 |
| M15 | Polynomial 2 nd order (combination of linear and interactive variables) | 5 features chosen previously, then repeated feature selection | 0.760 | 0.301 |
| M16 | Polynomial 2 nd order (combination of linear, squared and interactive variables) | 5 features chosen previously, then repeated feature selection | 0.781 | 0.248 |
| M17 | Multi-order | 5 features chosen previously, then repeated feature selection | 0.772 | 0.275 |
| M18 | Kernel | 5 features | 0.798 | 0.216 |
| M19 | Kernel | 21 features | 0.800 | 0.204 |
| M20 | BM2019 | 4 features | 0.686 | 0.512 |

RECOMMENDED MODELS

We have ranked the models according to three criteria: the MSE on the test set, their performance on case histories, and their trends when compared to the BM2019 model, which was selected due to its fast-growing usage in engineering practice. The ranking metrics can be found in Macedo et al. (2021). As previously discussed, models with a lower number of input

variables are desired from a practical perspective due to their simplicity. Hence, we recommend models with five features, which correspond to models M16, M15, M17, and M18. Model M1 can also be used when $T_s < 0.8$ s (beyond this range, the extrapolation can be problematic). Finally, model M6 can also be considered if only discrete estimates are desired, because it cannot provide continuous trends (e.g., see the trends for this model in Macedo et al., 2021).

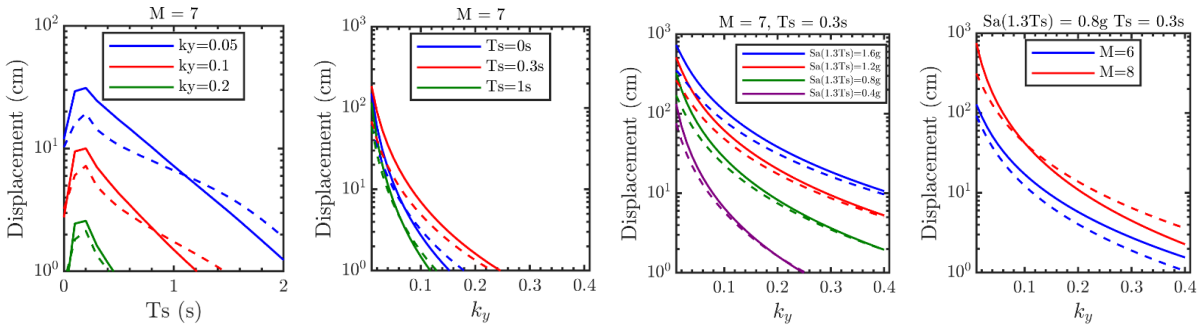


Figure 3. Model trends for the variations of k_y , T_s , $Sa(1.3 T_s)$, and M_w . Dashed lines: BM2019 model, solid lines: M16.

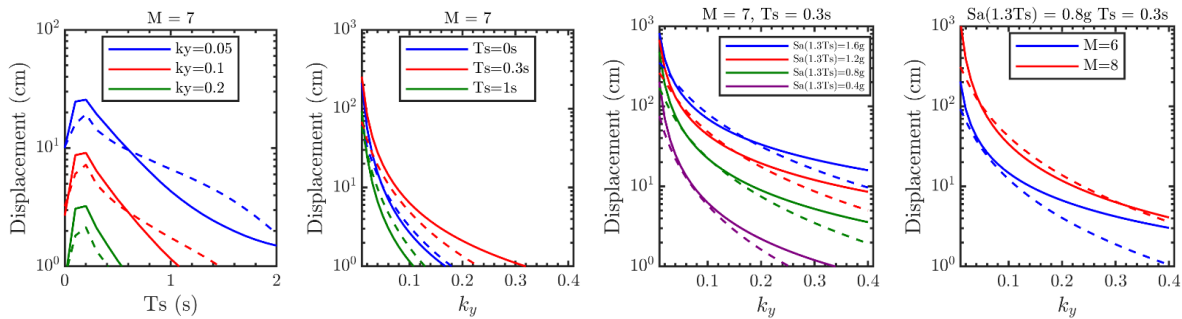


Figure 4. Model trends for the variations of k_y , T_s , $Sa(1.3 T_s)$, and M_w . Dashed lines: BM2019 model, solid lines: M17.

Table 2. Characteristics of the case histories of observed slope displacements

| Case | System | EQ | Observed D_{max} (cm) | k_y | T_s | M | $ClstD$ | V_{s30} |
|------|----------------------|--------------------|-------------------------|-------|-------|-----|---------|-----------|
| 1 | Buena Vista LF | 1989 Loma Prieta | None | 0.26 | 0.64 | 6.9 | 14.5 | 350 |
| 2 | Guadalupe LF | 1989 Loma Prieta | Minor | 0.20 | 0.64 | 6.9 | 20.1 | 760 |
| 3 | Pacheco Pass LF | 1989 Loma Prieta | None | 0.30 | 0.76 | 6.9 | 35.4 | 760 |
| 4 | Marina LF | 1989 Loma Prieta | None | 0.26 | 0.59 | 6.9 | 37 | 300 |
| 5 | Austrian Dam | 1989 Loma Prieta | 50 | 0.14 | 0.33 | 6.9 | 3 | 500 |
| 6 | Lexington Dam | 1989 Loma Prieta | 15 | 0.11 | 0.31 | 6.9 | 5 | 550 |
| 7 | Lopez Canyon C-A LF | 1994 Northridge | None | 0.27 | 0.64 | 6.7 | 8.4 | 600 |
| 8 | Lopez Canyon C-B LF | 1994 Northridge | None | 0.35 | 0.45 | 6.7 | 8.4 | 600 |
| 9 | Chiquita Canyon C LF | 1994 Northridge | 24 | 0.09 | 0.64 | 6.7 | 5 | 600 |
| 10 | Chiquita Canyon D LF | 1994 Northridge | 30 | 0.10 | 0.64 | 6.7 | 5 | 600 |
| 11 | Sunshine Canyon LF | 1994 Northridge | 30 | 0.31 | 0.77 | 6.7 | 7 | 600 |
| 12 | Oll Section HH LF | 1994 Northridge | 15 | 0.08 | 0.00 | 6.7 | 43 | 600 |
| 13 | Chabot Dam | 1906 San Francisco | Minor | 0.14 | 0.55 | 7.9 | 32 | 760 |

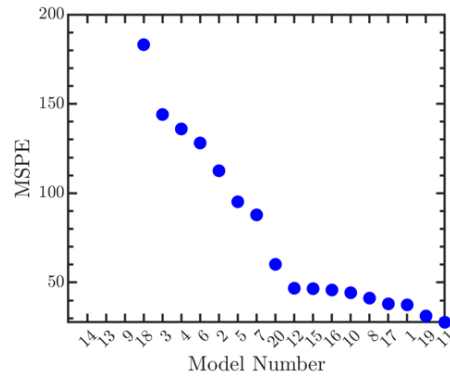


Figure 5. MSPE comparison based on estimations for the case histories.

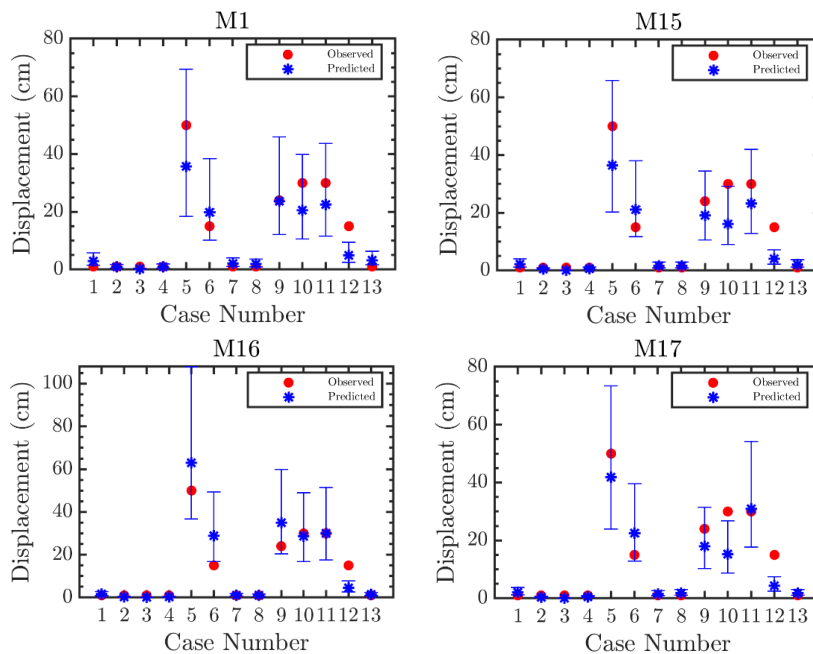


Figure 6. Performance of selected models on case histories (see Table 6 for the case histories details).

CONCLUSIONS

ML-based models can better capture the complex relationships between the inputs and response variable (i.e., seismically-induced displacements (D)) without restrictions to relatively simple functional forms as in traditional models formulated in the context of estimating D . With the current momentum in machine learning, the use of ML-based methods in performance-based earthquake engineering is appealing as also highlighted by previous efforts. In this study, we have proposed a new set of ML-based models to estimate D in slope systems affected by shallow crustal earthquakes using the NGA-West2 ground motion database. The selection of optimal features showed that k_y , T_s , M_w , PGV , and $Sa(1.3 T_s)$ are the optimal features for estimating D . we developed a total of 19 models using a variety of ML techniques (listed in Table 1), 12

models consider the five selected optimal features, and 7 additional models consider a full set of features for comparison purposes. In general, we observed that nonlinear models (e.g., Random Forest), generalized linear models, 2nd order polynomials, and kernel-based models showed higher prediction accuracies and lower MSE. On the other hand, PLSR, PCR, and 3rd-4th order polynomial models did not perform well. We also found that the performance of models with five features is comparable to the performance of models with a full set of features; hence, they have advantages for practical applications. We performed an overall assessment of the developed models considering MSE on the test set, their performance on case histories, and their trends for variations of slope properties, earthquake parameters, and IM_s . Based on this assessment, we recommend the following models: M16, M15, and M17, which correspond to polynomial-based models; and M18, which is a kernel-based model. We also recommend model M1 (a generalized linear model) when $T_s < 0.8$ s, and model M6 (Random Forest) can also be used, even though it cannot provide continuous estimates. The recommended models in this study can be used in engineering practice to evaluate the seismic performance of slope systems (through the estimation of D). These models also enhance the treatment of epistemic uncertainties in the estimation of D , which is desired given the scarcity of robust D models. Finally, the developed models have been integrated into the software SeismicHazard (Candia et al, 2019; Candia et al., 2018) for facilitating their use. The related scripts are available at: <https://github.com/fmc202/MLslopedisplacement>

REFERENCES

- APEGBC. (2010). *Guidelines for Legislated Landslide Assessments for Proposed Residential Development in British Columbia*. Association of Professional Engineers and Geoscientists of BC.
- Bozorgnia, Y., Abrahamson, N. A., Al Atik, L., Ancheta, T. D., Atkinson, G. M., et al. (2014). NGA-West2 research project. *Earthquake Spectra*; 30 (3): 973–987.
- Bray, J. D., and Travasarou, T. (2007). Simplified procedure for estimating earthquake-induced deviatoric slope displacements. *Journal of Geotechnical and Geoenvironmental Engineering, ASCE*; 133(4):381–392.
- Bray, J. D., and Macedo, J. (2019). Procedure for Estimating Shear-Induced Seismic Slope Displacement for Shallow Crustal Earthquakes. *Journal of Geotechnical and Geoenvironmental Engineering, ASCE*; 145(12), 04019106.
- Candia, G., Macedo, J., Jaimes, M. A., and Magna-Verdugo, C. (2019). A new state-of-the-art platform for probabilistic and deterministic seismic hazard assessment. *Seismological Research Letters*; 90(6):2262-2275.
- Candia, G., Macedo, J., and Magna-Verdugo, C. (2018). An integrated platform for seismic hazard evaluation. *11th US National Conference on Earthquake Engineering*; Los Angeles, USA.
- Cawley, G. C., Talbot, N. L., and Girolami, M. (2007). Sparse multinomial logistic regression via bayesian l1 regularisation. In: *Advances in neural information processing systems*; 209-216.
- Cho, Y. (2020). *Probabilistic assessment of the seismic performance of earth slopes using computational simulation* (Doctoral dissertation).
- Cho, Y., and Rathje, E. M. (2020). Displacement hazard curves derived from slope-specific predictive models of earthquake-induced displacement. *Soil Dynamics and Earthquake Engineering*; 138, 106367.

- FHWA. (2011). LRFD Seismic Analysis and Design of Transportation Geotechnical Features and Structural Foundations. Geotechnical Engineering Circular No. 3, Report No. FHWA-NHI-11-032, 592 p.
- Hastie, T., Tibshirani, R., and Friedman, J. (2009). *The elements of statistical learning: data mining, inference, and prediction*. Springer Science & Business Media.
- ICC (International Council Code). (2015). *International building code*. Washington, DC: International Code Council.
- Krishnapuram, B., Carin, L., Figueiredo, M. A., and Hartemink, A. J. (2005). Sparse multinomial logistic regression: Fast algorithms and generalization bounds. *IEEE transactions on pattern analysis and machine intelligence*; 27(6):957-968.
- Macedo, J., Liu, C., and Soleimani, F. (2021). Machine-learning-based predictive models for estimating seismically-induced slope displacements. *Soil Dynamics and Earthquake Engineering*, 106795.
- Macedo, J., Candia, G., Lacour, M., and Liu, C. (2020). New developments for the performance-based assessment of seismically-induced slope displacements. *Engineering Geology*; 277, 105786.
- Macedo, J., and Candia, G. (2020). Performance-based assessment of the seismic pseudo-static coefficient used in slope stability analysis. *Soil Dynamics and Earthquake Engineering*; 133, 106109.
- Macedo, J. L. (2017). *Simplified procedures for estimating earthquake-induced displacements*. Ph.D. thesis, Dept. of Civil and Environmental Engineering, Univ. of California, Berkeley.
- Macedo, J., Bray, J., and Travararou, T. (2017). Simplified procedure for estimating seismic slope displacements in subduction Zones. *16th World Conference on Earthquake*.
- MEM. (1997). Guía ambiental para la estabilidad de taludes de depósitos de desechos sólidos de mina. Ministerio de energía y minas.
- Ministerio de Minería (2007). Reglamento para la aprobación de proyectos de diseño, construcción, operación y cierre de los depósitos de relaves. Retrieved from <http://bcn.cl/1uvyi>. (In spanish).
- Moreno, J. J., and Kendall, S. (2019). Considerations for preparing design criteria for dewatered tailings facilities. *6th international seminar in Tailings Management*.
- Rathje, E. M., and Saygili, G. (2008). Probabilistic Seismic Hazard Analysis for the Sliding Displacement of Slopes: Scalar and Vector Approaches. *Journal of Geotechnical and Geoenvironmental Engineering, ASCE*; 134(6).
- Rathje, E. M., and Bray, J. D. (1999). An examination of simplified earthquake-induced displacement procedures for earth structures. *Canadian Geotechnical Journal*; 36(1):72–87.
- Xie, Y., Ebad Sichani, M., Padgett, J. E., and DesRoches, R. (2020). The promise of implementing machine learning in earthquake engineering: A state-of-the-art review. *Earthquake Spectra*; 36(4):1769-1801.
- Wang, M. X., Huang, D., Wang, G., and Li, D. Q. (2020). SS-XGBoost: a machine learning framework for predicting newmark sliding displacements of slopes. *Journal of Geotechnical and Geoenvironmental Engineering*; 146(9):04020074.